Supporting Information

The Mechanism of Hydrogen Adsorption on Transition Metal Dichalcogenides as Hydrogen Evolution Reaction Catalyst

Jinsong Wang, Jia Liu, Bao Zhang, Xiao Ji, Kui Xu, Chi Chen, Ling Miao*, Jianjun Jiang*

School of Optical and Electronic Information, Huazhong University of Science and Technology,

Wuhan 430074, PR China

* Corresponding author E-mail: miaoling@mail.hust.edu.cn; jiangjj@mail.hust.edu.cn

Table S1. Calculated values of 2D single-layer MX_2 in the H and T Structures: conduction band minimum, E_{cv}; free energy of hydrogen adsorption, ΔG_H; and conductivity of MX_2 (S and M indicating semiconductor and metallicity separately).

| MX_2	phase	Conductivity(S/M)	E_{cv}	ΔG_H (eV)
MoS_2	H	S	-4.06	1.96
	T	M	-5.03	0.12
ScS_2	H	S	-5.46	-0.12
	T	M	-6.78	-0.81
TiS_2	H	S	-6.01	-0.11
	T	M	-5.71	0.34
VS_2	H	M	-5.89	0.14
	T	M	-5.43	0.04
CrS_2	H	S	-4.62	1.13
	T	M	-5.11	-0.17
CoS_2	H	M	-5.15	-0.12
	T	M	-5.94	-0.08
NiS_2	H	M	-5.08	0.61
	T	S	-5.17	0.58
ZrS_2	H	S	-5.76	0.04
	T	S	-5.27	0.85
HfS_2	H	S	-5.55	0.22
	T	S	-5.29	1.08
WS_2	H	S	-3.86	2.11
	T	M	-4.89	0.22
FeS_2	H	M	-5.24	0.31
	T	M	-5.39	0.27
NbS_2	H	M	-6.09	0.09
	T	M	-5.37	0.21
$MoSe_2$	H	S	-3.62	2.11
	T	M	-4.52	0.61
$CoSe_2$	H	M	-5.35	0.43
	T	M	-5.47	0.49
$ScSe_2$	H	M	-5.81	0.26
	T	M	-6.24	-0.34
$HfTe_2$	H	S	-5.13	0.76
	T	M	-4.66	1.33
$CoTe_2$	H	M	-5.01	0.78
	T	M	-4.97	0.61
$MoTe_2$	H	S	-3.53	2.15
	T	M	-4.15	0.93

Table S2. Calculated Values of non-metallic elements doped 2H-MoS$_2$: The Formation energy, E$_f$; energy of states-filling site, E$_{cv}$; free energy of hydrogen adsorption, ΔG_H;

| | E$_{form}$ (eV) | | E$_{cv}$ | ΔG_H (eV) |
	Mo-rich	S-rich		
B-MoS2	2.35	4.46	-5.47	0.58
C-MoS2	-0.58	1.53	-4.60	1.04
N-MoS2	0.44	2.57	-5.23	0.73
O-MoS2	-2.76	-0.64	-4.05	1.88
F-MoS2	-1.65	0.47	-4.19	1.33
P-MoS2	0.42	2.55	-5.65	0.39
Se-MoS2	-1.23	0.89	-4.02	1.90
S-vacancy	1.08	3.03	-4.58	1.31
2S-vacancies	1.12	3.18	-4.72	1.27
3S-vacancies	1.22	3.28	-4.86	1.21
4S-vacancies	1.26	3.32	-4.97	1.10

Figure S1. Calculated DOS and E_{cv} for 2H- and 2T-phase MoX$_2$ (X=S, Se, Te). Watchet and yellow indicate the filled scope of electrons. Red dashed line is set to be E_{cv}.
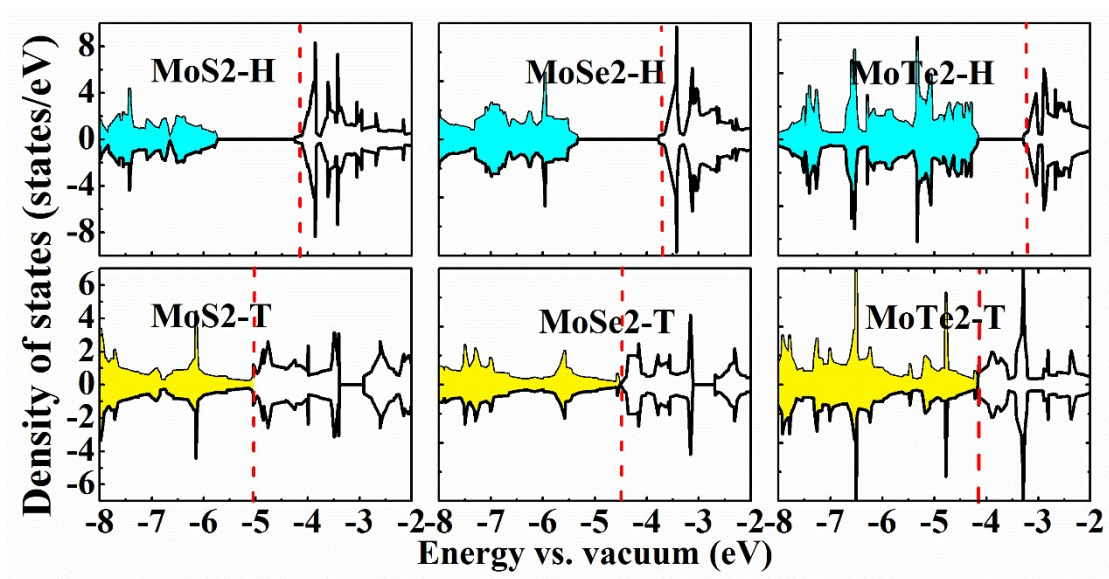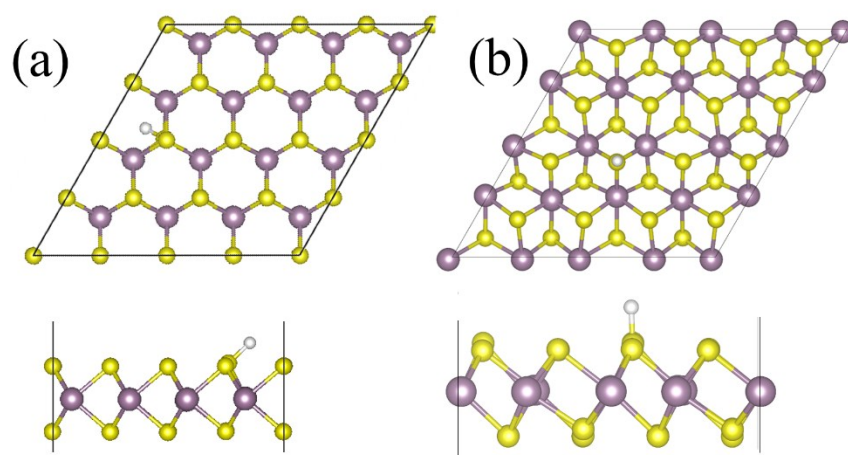
Figure S2. Calculated DOS and E_{cv} for 2 × 2 supercell of 2H- and 2T-phase TMDs. Watchet and yellow indicate the filled scope of electrons. Red dashed line is set to be E_{cv}.
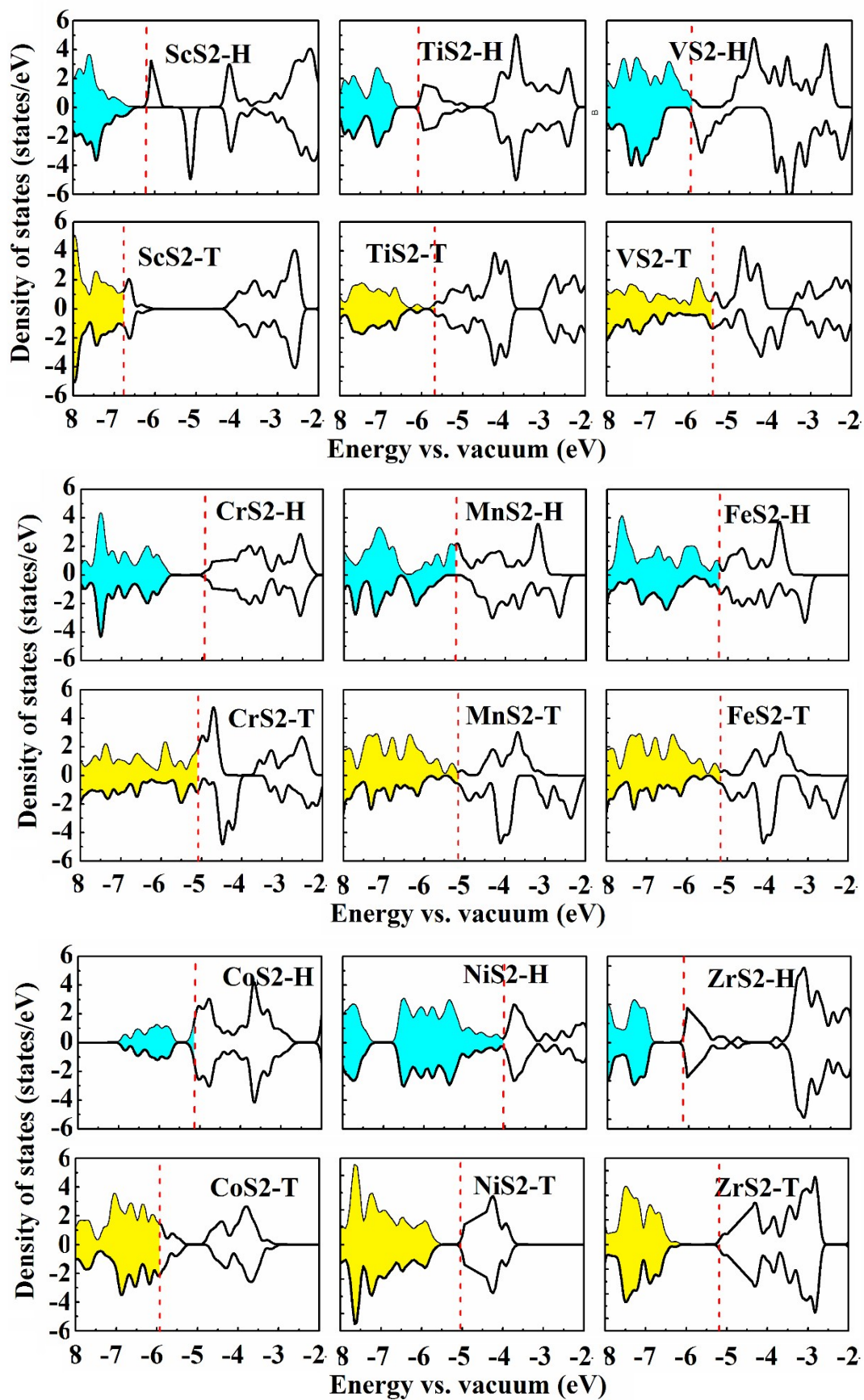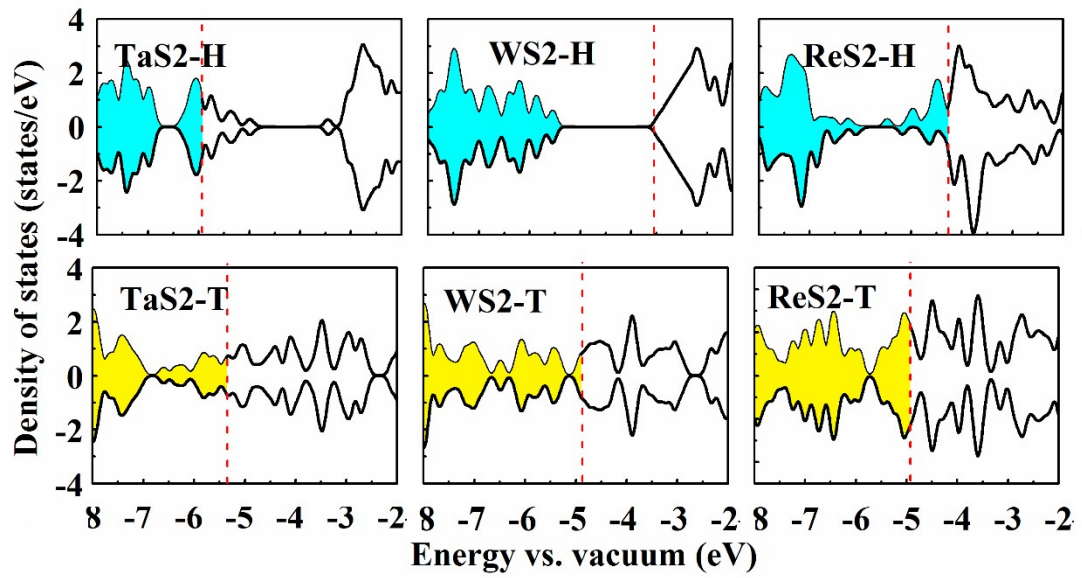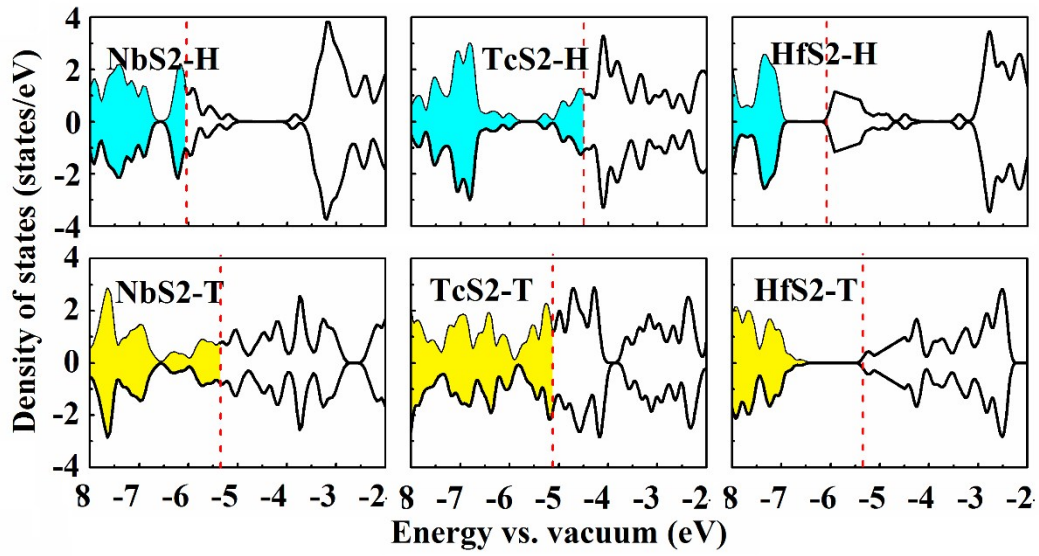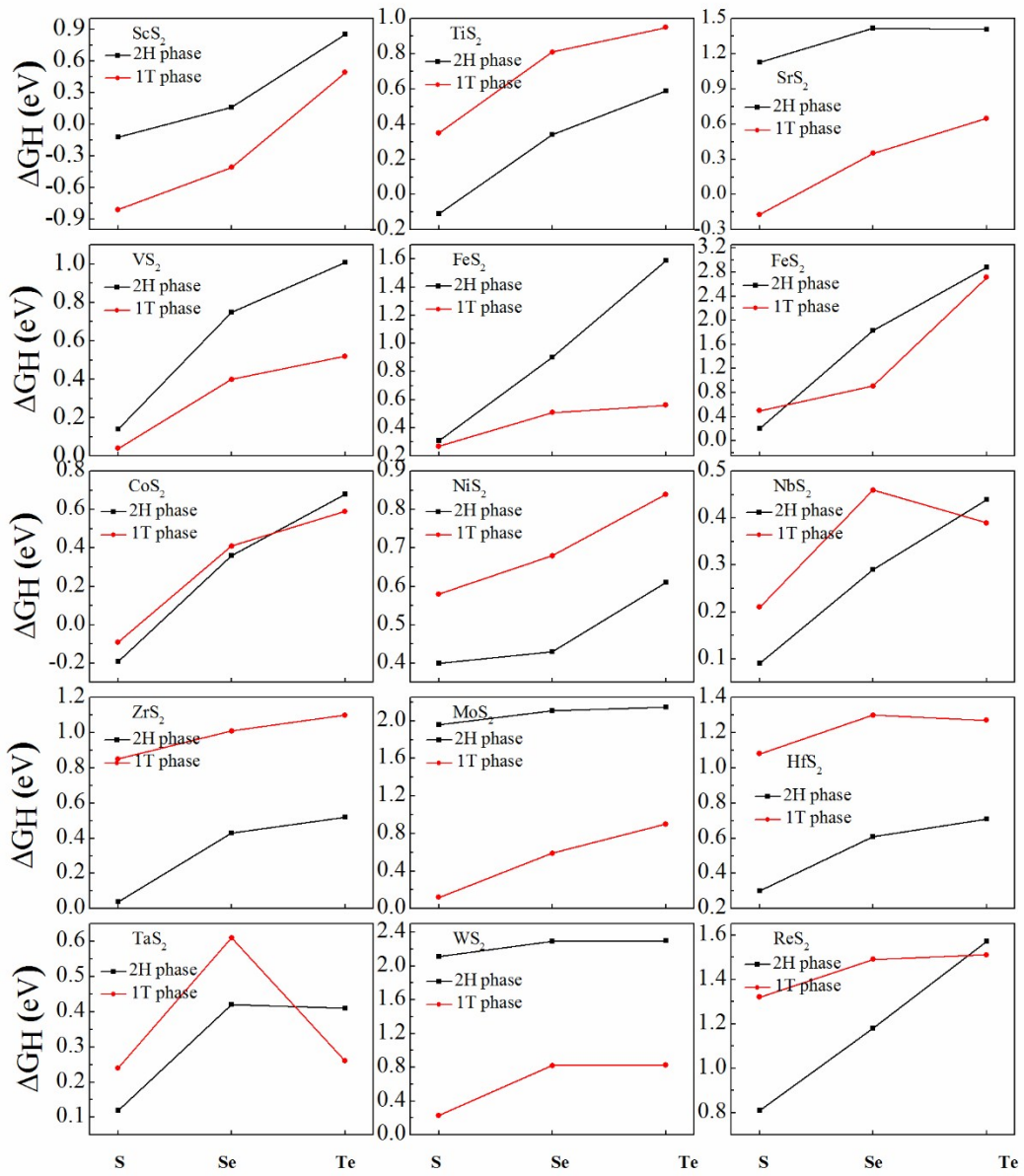
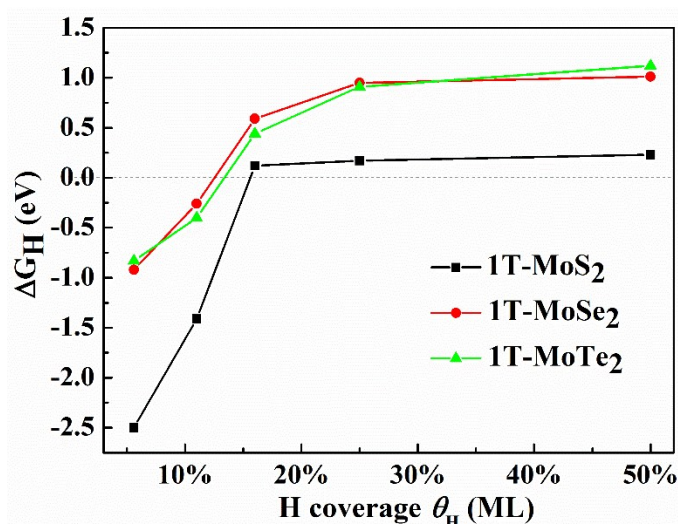**Figure S3.** Geometric structure of (a) H-phase and (b) T-phase after adsorb H.

**Figure S4.** The variation of hydrogen chemisorption energy of MX2 with different Chalcogen.

Figure S5. The change in hydrogen adsorption free energy ΔG_H as a result of coverage for representative 1T-phase MoX$_2$ (X=S, Se and Te).


Hydrogen coverage dependence of ΔG_H. Hydrogen coverage as determinant of ΔG_H has been discussed in the present work [1-2]. Take T-phase MoS$_2$, MoSe$_2$ and MoTe$_2$ as an example in Figure 4S, generally, the hydrogen binding strengthens incrementally as the hydrogen coverage decreases, it is noticeable that ΔG_H possess extraordinary large negative value, it is similar to Tang et al's reports [2]. One important factor is 1T-phase structurally transforms to the 1T′ once H is adsorbed when the hydrogen coverage lower than 25% (Figure S3) [3-4]. Moreover, the ΔG_H does not decrease solely with the increasing hydrogen coverage due to the different deformation degree in geometry because of the surface reconstitution when hydrogen is adsorbed [4]. Combined with Figure 3, under lower hydrogen coverage, it is most likely that the hydrogen adsorption is closer to equilibrium when filling level approach to SHE.

Figure S6. Calculated DOS and E_{cv} of heteroatom doped 2H-phase MoS$_2$. Red line is set to be E_{cv} black dashed lines indicate standard hydrogen electrode SHE.
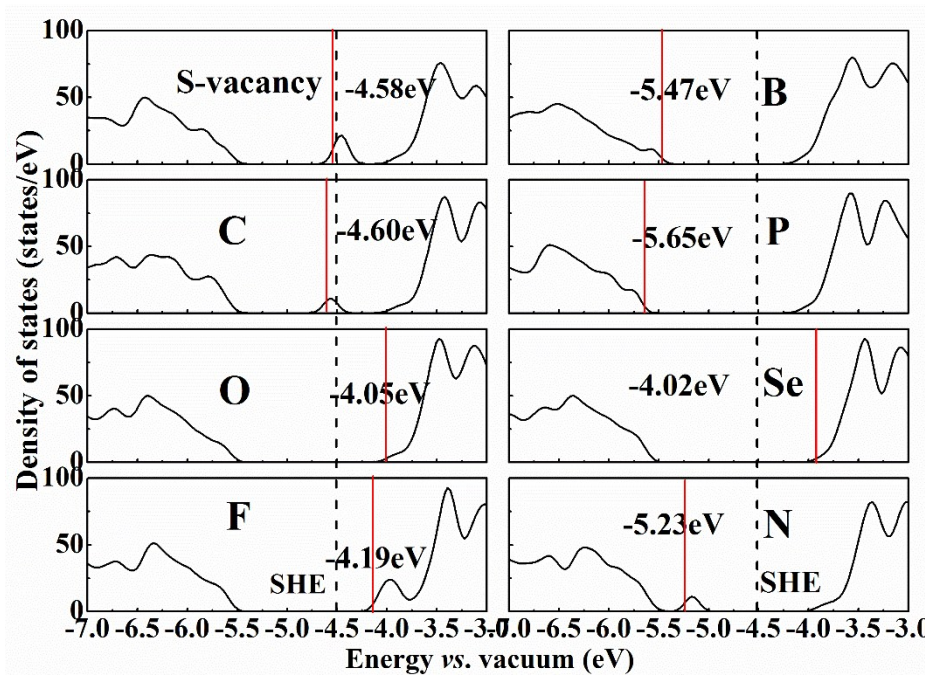
Figure S7. PDOS of S without (up) and with (middle)adsorbed H for heteroatom doping. (a) pristine (b) B-doping, (c)C-doping, (d) N-doping, (e) F-doping, (f) S-vacancy. One new peaks near the Fermi level are introduced on S *p* orbital due to the inducing of doping, then the peak disappear after S atom absorb H.
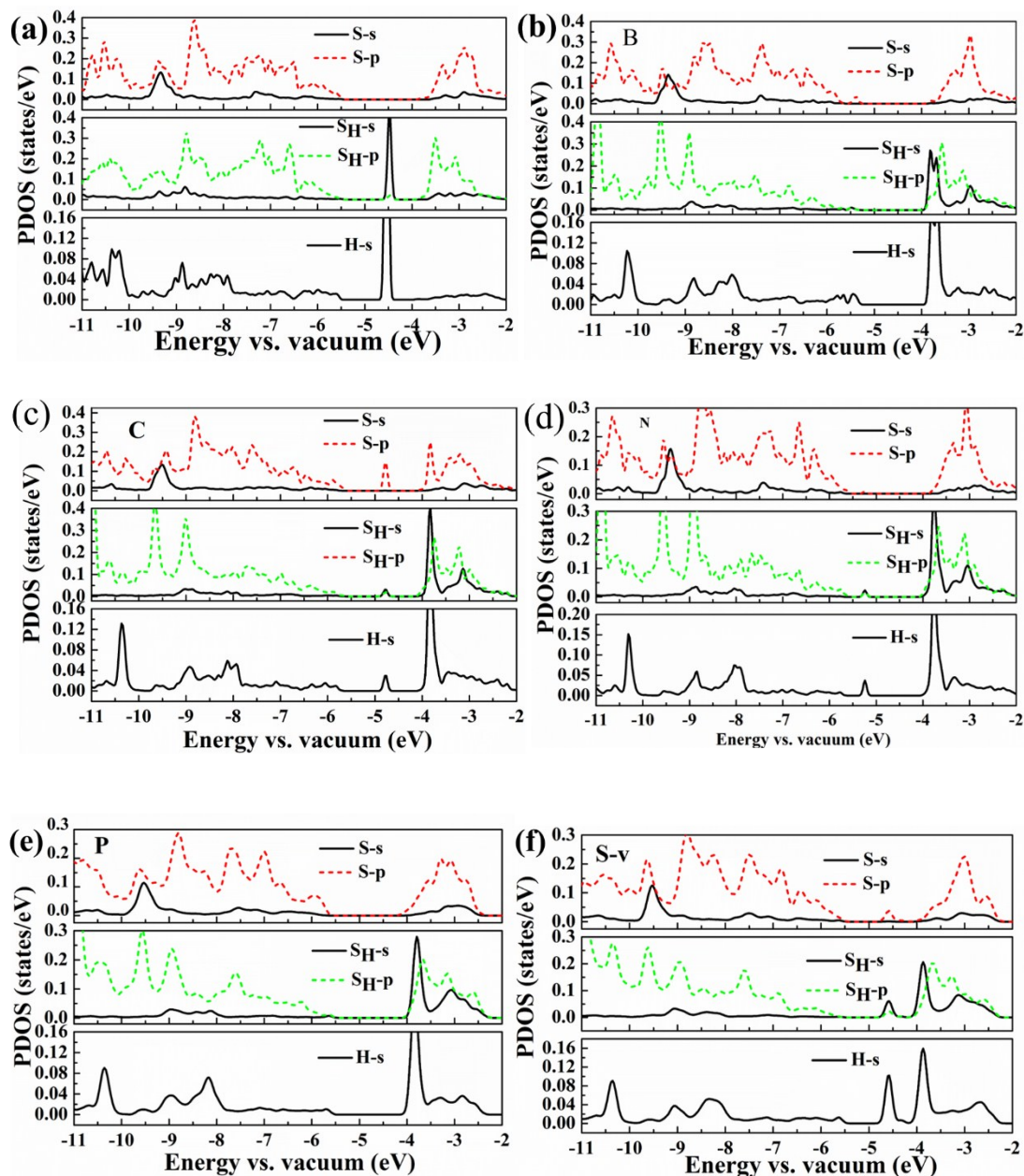

The impurity levels are disparate, for the p-type doping such as B, P and N which the impurities are close to CBM lower than SHE, there show hybridization between S *p* and H s orbits with the different heteroatom substitution for S (Figure S5, S6), suggesting that it more easily to fill the H electron. On the contrary, for n-type doping and pristine MoS_2 which the lowest unoccupied states high than SHE, indicating the unsubstantial covalent bond due to the weaker hybridizing of H s and S p orbitals, demonstrating the sluggish kinetics of hydrogen adsorption. In general, the H electron can be accommodated easily as the impurity states located on lower energies level, which explains the gradual strengthening of H binding seen earlier, in good agreement with 'states-filling' mode.

Figure S8. The Charge density different for heteroatom doping. (a) B-doping, (b) C-doping, (c)

N-doping, (d) P-doping. the red and green areas stand for election gain and loss, respectively.
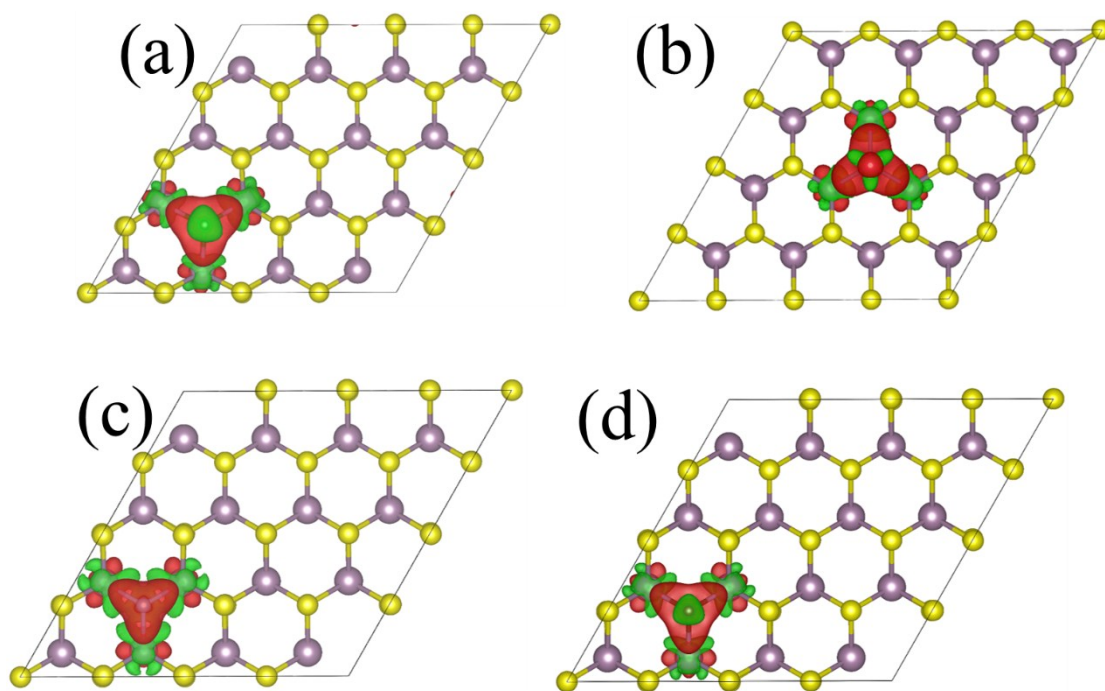
Figure S9. Computational electronic band structure of monolayer 2H-phase MoS$_2$ with different S

vacancies.
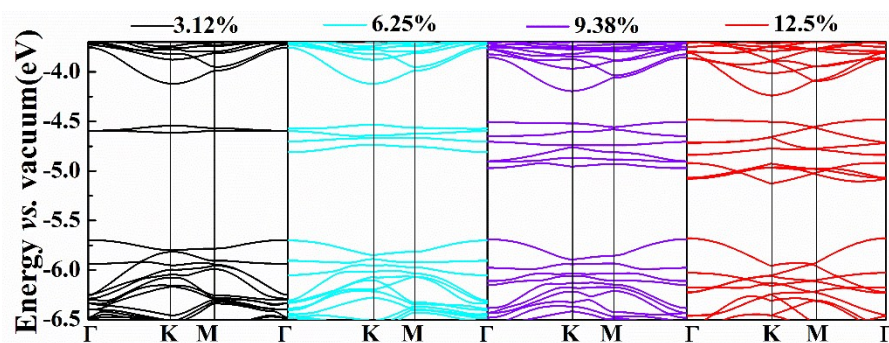
References

[1] Tsai, C.; Chan, K.; Nørskov, J. K.; Abild-Pedersen, F., Theoretical Insights into the Hydrogen Evolution Activity of Layered Transition Metal Dichalcogenides. *Surf. Sci.* **2015**, *640*, 133-140.

[2] Tang, Q.; Jiang, D.-e., Mechanism of Hydrogen Evolution Reaction on 1t-Mos2from First Principles. *ACS. Catal.* **2016**, *6*, 4953-4961.

[3] Tang, Q.; Jiang, D.-e., Stabilization and Band-Gap Tuning of the 1t-Mos2monolayer by Covalent Functionalization. *Chem. Mater.* **2015**, *27*, 3743-3748.

[4] Gao, G.; Jiao, Y.; Ma, F.; Jiao, Y.; Waclawik, E.; Du, A., Charge Mediated Semiconducting-to-Metallic Phase Transition in Molybdenum Disulfide Monolayer and Hydrogen Evolution Reaction in New 1t' Phase. *J. Phys. Chem. C* **2015**, *119*, 13124-13128.